Tuning the Diameter of Single-Walled Carbon Nanotubes by Temperature-Mediated Chemical Vapor Deposition

5 AUTHORS, INCLUDING:

Yagang Yao
Chinese Academy of Sciences
59 PUBLICATIONS   **1,334** CITATIONS

SEE PROFILE

Xiaochuan Dai
Harvard University
8 PUBLICATIONS   **121** CITATIONS

SEE PROFILE

Jin Zhang
Peking University
160 PUBLICATIONS   **4,680** CITATIONS

SEE PROFILE

Tuning the Diameter of Single-Walled Carbon Nanotubes by Temperature-Mediated Chemical Vapor Deposition

Yagang Yao, Xiaochuan Dai, Ran Liu, Jin Zhang,* and Zhongfan Liu*

Beijing National Laboratory for Molecular Sciences (BNLMS), Key Laboratory for the Physics and Chemistry of Nanodevices, State Key Laboratory for Structural Chemistry of Unstable and Stable Species, College of Chemistry and Molecular Engineering, Peking University, Beijing 100871, P.R. China

In the present study, we systematically described the tuning of the diameter of single-walled carbon nanotubes (SWNTs) from individual catalyst particle by temperature-mediated chemical vapor deposition (CVD). The basic idea is to change the temperature quickly during the growth of ultralong SWNTs via a "kite mechanism". It has been found that the diameter of a SWNT varied with temperature oscillation; higher temperature led to thinner SWNTs with the same catalyst particle and lower temperature led to thicker ones. These diameter variations of SWNTs were measured by resonance Raman spectroscopy and atomic force microscopy (AFM). It has also been found that the diameter changes were highly related to their initial diameters. For each initial diameter, there are various probabilities of different diameter changes, but all of them are below a certain maximum, which depends on the initial diameter. The maximum diameter change reaches an extremum of 0.40 nm, while the initial diameter is around 1.6 nm, and the maximum diameter changes are much lower for nanotubes with a larger or smaller diameter, which implies that the diameter mediation by temperature is limited. Based on the results, a well-aligned individual ultralong SWNT array with a narrow diameter distribution of small diameter (around 1.0 nm) or larger diameter (around 2.0 nm) could be grown by ascending or descending temperature-mediated CVD, respectively. At the same time, a simple growth model supposing there is a graphene transition state when the tube formation is initiated is proposed to explain these phenomena. Under this model, the relationship between the growth temperature and the diameter of SWNTs was calculated. It has been found that, a catalyst particle with certain mole fraction of carbon will produce SWNTs with smaller diameter under higher growth temperature and vice versa. This trend accords well with our experimental data. Such diameter modulation of SWNTs by temperature would also help us to understand the CVD growth mechanism of SWNTs.

Introduction

Single-walled carbon nanotubes (SWNTs) possess superior electronic and physical properties that provide many potential applications in electronics, optics, sensing and other fields.[1,2] They can be metallic or semiconducting determined by their diameter and chiral angle, both of which can be described by a pair of indices (n,m), called the chiral vector. Most importantly, the band gap in semiconducting SWNTs is inversely proportional to the tube diameter and approaches zero at large diameters.[3] Hence, in order to realize the application of SWNTs in nanoelectronic devices, it is crucial to control the diameters of SWNTs.

There are several techniques to produce SWNTs, including arc discharge,[4,5] laser ablation,[6] and chemical vapor deposition (CVD).[7] Among these synthesis routes, CVD could be considered as one of the best methods for low-cost and large-scale synthesis of high-quality nanotube materials.[8] Besides, the nanotubes could be grown on the desired substrates[9] required for application or further investigation. In addition, the growth positions[10,11] are controllable by careful deposition of the catalyst, and no other growth methods have been developed to produce vertically or horizontally aligned nanotubes on a substrate.[12,13]

Although the CVD method provides the way to highly controlled SWNT production, it has not yet been developed to the degree of controlling their unique electrical properties because common as-synthesized SWNTs consist of nanotubes with wide variety both in diameter and in chirality. At the moment, many intensive efforts have been focused on postproduction separation methods[14,15] to obtain unique structure of SWNTs, including gas-phase plasma etching,[16] laser irradiation,[17] xenon-lamp irradiation,[18] electrical breakdown of m-SWNTs,[19] the selective separation of DNA-wrapped[20−22] or cosurfactant-encapsulated carbon nanotubes,[23,24] and electrophesis.[25] However, these methods always involve further solution treatment or etching processes, which inevitably impair the carbon nanotubes. It is therefore desirable to invent a new method for accurate and scatheless control of the diameter of CVD-grown SWNTs.

In order to control the diameter of the SWNTs, many factors should be considered, including the size of catalyst particle,[26,27] carbon feeding rate,[28] type of carbon sources,[29−31] and so on. First, since it is believed that the diameters of the SWNTs are related to the size of the metal particles, great efforts are being made to obtain narrower diameter distribution catalyst nanoparticles, including iron(III) ions loaded into inversed micelles formed by block copolymers,[32,33] identical metal-containing molecular nanoclusters,[34] controllable amounts of iron(III) into the cores of apoferritin, polyamidoamine dendrimers as carriers

* To whom correspondence should be addressed. Tel & Fax: 86-10-6275-7157. Email: jinzhang@pku.edu.cn.

to deliver complex iron(III) ions uniformly onto silicon oxide substrates,[35,36] cobalt-substituted MCM-41 molecular sieves,[37,38] Fe/MgO catalyst,[39] etc., as the preorganized catalyst source. Despite that, many researchers have found that the final size of catalyst particles vary greatly, even larger than the distribution of diameters of SWNTs grown from them. Besides, in the process of SWNTs growth, the diameters of catalyst nanoparticles might also be influenced by conglomeration at high temperature.[40] Thereby, it might be oversimplified to accept the idea that the SWNT diameter is determined only by the size of catalyst particles. Second, Lu et al. believed the diameters of SWNTs were tightly related to the carbon feeding rate due to selective activation of nanoparticles and the diameters could be controlled even when highly polydisperse nanoparticles were used as catalyst.[28] Feng et al. also put forward that the synthesis of uniform SWNTs was highly related to an ultralow carbon feeding rate and high hydrogen flow rate.[41] Third, another different approach developed by a team of researchers in Rice University is cutting a single *n,m*-type nanotube into many short segments, docking them with catalyst particles, and then using them as templates for further growth.[42] Those secondary grown nanotubes are expected to be of the same diameter and type as the original ones, but further characterization and improvements in yield are still needed. Apart from these methods, plenty of other strategies have also been reported in the literature. Among those parameters, however, which one is the crucial factor to determine tube diameter is still not clear.

In this work, we followed the growth process of an individual SWNT from certain catalyst nanoparticles under gas flow directed growth mode (kite mechanism), and investigated the modulation of diameters of SWNTs through temperature oscillation. We found that the diameter of a SWNT varied when temperature changed; higher temperature led to thinner SWNTs with the same catalyst particle and lower temperature led to thicker ones.[43] Following this idea, we measured and analyzed the diameter changes of 62 nanotubes and found that the extents of the changes were related to the original diameters. The diameters vary slightly for quite thin and quite thick nanotubes and vary remarkably by 0.40 nm for nanotubes with diameters around 1.6 nm, indicating that the modulation of diameters through temperature is finite. Based on the results, a well-aligned individual ultralong SWNT array with a narrow diameter distribution of small diameter (around 1.0 nm) and larger diameter (around 2.0 nm) can be grown by ascending or descending temperature-mediated CVD, respectively, and this kind of array will show its potential value in further application in devices.[1,2] At the same time, a simple growth model supposing that there is a graphene transition state when the tube formation is initiated was proposed to explain these phenomena. Under this model, the relationship between the growth temperature and the diameter of SWNTs was calculated. We found that a catalyst particle with certain mole fraction of carbon would produce SWNTs with smaller diameter under higher growth temperature and larger diameter under lower growth temperature, which accords well with our experimental data. Such diameter modulation of SWNTs by temperature would help us to understand the CVD growth mechanism of SWNTs.[44]

Experimental Section

A. Choosing the Growth Mode of SWNTs. It is well-known that the diameters of SWNTs are closely related to many growth factors. Thus, if we want to investigate the effect of temperature on the diameters of SWNTs from a certain catalyst nanoparticle, the effect of other growth parameters should be

eliminated. For this purpose, hence, it is important to choose a suitable experimental system to separate the effect of temperature from that of other factors. Luckily there was a breakthrough in 2003 made by Liu's group[12] and developed by other research groups later.[43,45−50] They grew millimeter-long, even centimeter-long, horizontally aligned SWNTs on flat substrates and proved that catalyst nanoparticles at the tip of a SWNT could fly over barriers or trenches, which is described as the "kite mechanism". In this mechanism, after the nanotubes grow upward upon the surface, they are captured by the wind of the gas flow, which will eventually lead to an aligned and continuous growth.[51] Thereby, this system is appropriate for our research purpose about SWNT growth mediated by temperature because it can remove the complicated interaction between catalyst nanoparticles and the substrate, catalyst conglomeration when the particles meet on the substrate at high growth temperature, etc. At the same time, an individual ultralong SWNT grown by this method is easy to be characterized by Raman spectroscopy[52−54] and AFM.

B. Growth Parameters of Ultralong SWNT Arrays. Ultralong SWNTs were synthesized using ethanol as the carbon source and Fe as catalyst. Silicon wafers with an 800 nm silica layer were used as the substrates, which is propitious to get a stronger intensity of resonant Raman signal of the SWNT than that of a SWNT on silicon substrates. $Fe(OH)_3$ colloids prepared by hydrolyzing of $FeCl_3$ in boiling water[18] or a ferritin diluted 1:100 (v/v) with deionized (DI) water worked as catalyst solution and were applied to one edge of a SiO_2/Si substrate by microcontact printing. The substrate with the catalyst precursor was then placed in a horizontal 3.7 cm quartz tube furnace while the catalyst end faced the gas flow. The catalyst precursor was prereduced in flowing Ar/H_2 (500 sccm/30 sccm) gas mixture at 900 °C for 10 min, and then ethanol vapor was introduced into the furnace by bubbling 200 sccm Ar through the ethanol. In the end, the reactor was purged with Ar/H_2 (500 sccm/30 sccm) and cooled down to room temperature. Experiments included growth processes under constant temperature (900, 920, 940, or 960 °C), one-time temperature change (from 900 to 950 °C or from 950 to 900 °C), two-time temperature changes (from 900 to 950 °C then back to 900 °C or from 950 to 900 °C then back to 950 °C), and ascending/descending temperature schedule (shown in Figure 4a and Figure 6a, respectively). Typically the temperature oscillation between 900 and 950 °C shown in Figure S1, Supporting Information usually takes 35−40 s.

C. Characterization Methods. We made the patterned markers by photolithography and wet etching to locate the SWNTs on SiO_2/Si substrate. That makes it convenient for us to recognize and address any SWNT on the surface. Scanning electron microscopy (SEM, Hitachi S4800 field emission, Japan), micro-Raman spectroscopy (Renishaw 1000) assembled with a confocal imaging microscope, with an excitation energy of 1.96 eV (632.8 nm) and a 1 μm excitation spot size, and atomic force microscopy (AFM, Veeco NanoScope III, Veeco Co., USA, operated at tapping-mode) were used to characterize the as-produced ultralong SWNTs.

Results and Discussion

A. The Relationship between the Diameter of SWNTs and Growth Temperature. Typical SEM images of ultralong SWNT arrays are shown in Figure 1a−c for our experiments of growth processes under constant temperature at 960 °C (Figure 1a), monotone ascending (Figure 1b), and descending (Figure 1c) sequence of temperature. It is clear to see that well aligned parallel individual ultralong SWNTs were obtained on the SiO_2/Si substrates at any temperature between 900 and 1020

Tuning Diameter of Single-Walled Carbon Nanotubes

J. Phys. Chem. C, Vol. 113, No. 30, 2009 **13053**
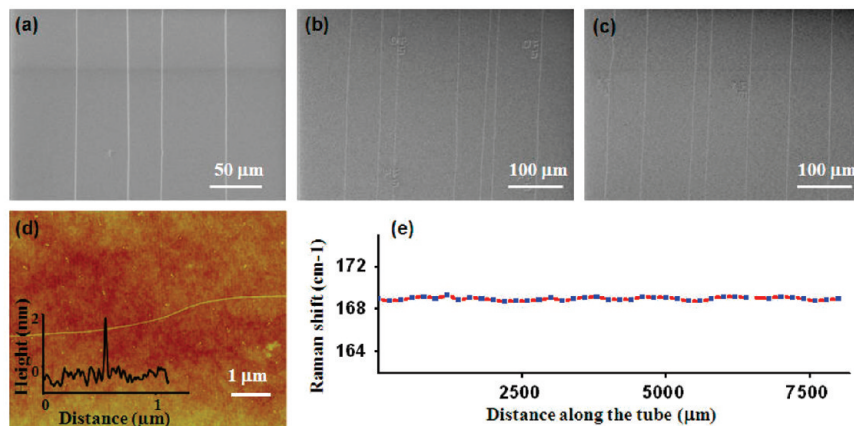
Figure 1. Typical SEM images of ultralong SWNT arrays grown under constant temperature at 960 °C (a), monotone ascending (b), and descending (c) sequence of temperature. It is clear to see the patterned markers in the images and thus any SWNT on the substrate can be identified. In these images, we found that there is hardly any termination of the growth of ultralong SWNTs observed in our system. (d) AFM image of a segment of an ultralong SWNT, and its section analysis is presented in the inset. (e) RBM signals along an 8.0 mm long nanotube.
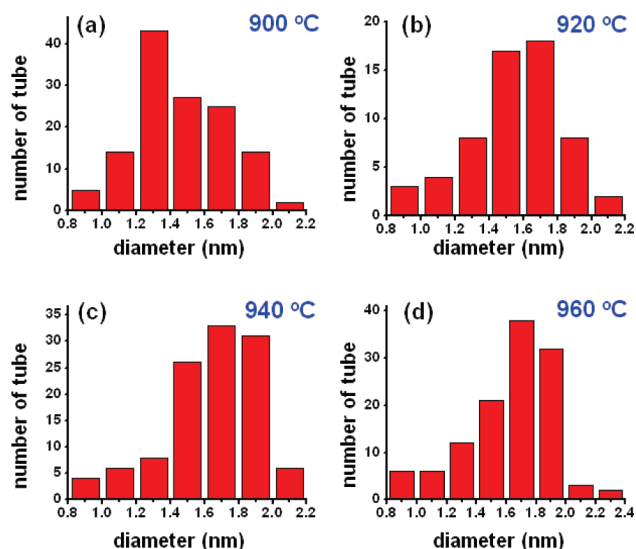
Figure 2. SWNT diameter distributions grown at 900 (a), 920 (b), 940 (c), and 960 °C (d). The mean diameters of SWNTs are 1.45 (a), 1.51 (b), 1.53 (c), and 1.57 nm (d).

°C under our experiment conditions. The length of ultralong SWNT is only limited by the substrate size, the hot zone of the furnace, and the growth time.

With regard to the SWNT growth under constant temperature at 960 °C, AFM (Figure 1d) and Raman spectroscopy (Figure 1e) characterization data along the nanotubes were collected to prove that the diameter would remain unchanged along their length. The inset in Figure 1d, an example of section analysis of the nanotube presented in Figure 1d, shows a constant diameter at 2.0 nm. Raman radial breathing mode (RBM) signals, which are related to the diameter of SWNTs via the equation[55] $d = 248 \text{ cm}^{-1}/\omega_{RBM}$, where ω_{RBM} is the RBM frequency, were collected along an 8.0 mm long nanotube (Figure 1e). The constant Raman shifts reinforce the conclusion that the diameter of the tube is still unvaried.

Then, we mapped a few dozen SWNTs along the line 2.0 mm away from the catalyst zone via Raman spectroscopy, and the results are displayed in Figure 2. The SWNTs were grown under a constant temperature of 900, 920, 940, or 960 °C. It can be seen that the mean diameter of SWNTs increased from 1.45 to 1.57 nm when the growth temperature increased from 900 to 960 °C, which could be explained by higher probability

of catalyst nanoparticle agglomeration at the higher temperature.[40] Nevertheless under different constant growth temperature, the diameter of nanotubes will still not change.

However, in our last paper, by changing the temperature during the growth, we found that an individual SWNT varied its diameter even though the catalyst particle remained the same.[43] Now we have synthesized 1000 nanotubes and measured 62 of them by Raman, because the RBM signals are mostly undetectable while the SWNT's electronic transition energy, E_{ii}, does not match the energy of the laser,[56,57] which is 1.96 eV. Hence, we spent years to collect the Raman data, part of which is arrayed in Table S1, Supporting Information. We analyzed those data with temperature change of 50 °C and found that the diameter changes are highly related to the initial diameters of the SWNTs (the relationship is shown in Figure 3). From Figure 3, we could determine that for each initial diameter, there are various probabilities of different diameter changes, but all of them are below a certain maximum, which depends on the initial diameter. As shown in Figure 3a, in the ascending temperature experiments, the maximum diameter change increases along with the initial diameter, reaches an extreme of 0.40 nm when the initial diameter is around 1.63 nm, and then declines after the peak. Correspondingly, in the descending temperature experiments (in Figure 3b), the curve shape remains unvaried and the extreme point is at about 1.61 nm. That implies that the diameter mediation with temperature is limited.

B. Growth of Ultralong SWNT Arrays with Narrow Diameter Distribution by Monotone Ascending or Descending Temperature-Mediated CVD. As discussed above, the SWNTs with a diameter around 1.6 nm vary most remarkably when the growth temperature changes, but the SWNTs with an obviously larger or smaller diameter vary little correspondingly. Based on this result, the diameter distribution will contract and centralize at a small diameter, because when we increase the growth temperature persistently, (1) the SWNTs with a diameter around 1.2 nm will hardly change their diameters obviously, (2) the SWNTs with a diameter from 1.4 to 1.6 nm will decrease their diameter by 0.1−0.4 nm and thus their final diameters will converge to about 1.2 nm, (3) the SWNTs with a diameter slightly larger than 1.6 nm will first approach 1.6 nm at an increasing speed and then move to around 1.2 nm rapidly as the nanotubes with an initial diameter about 1.6 nm do, and (4) the SWNTs with a quite large diameter will also approach to 1.6 nm at an increasing speed and widely distribute in various diameters if their diameters do not diminish fast enough to
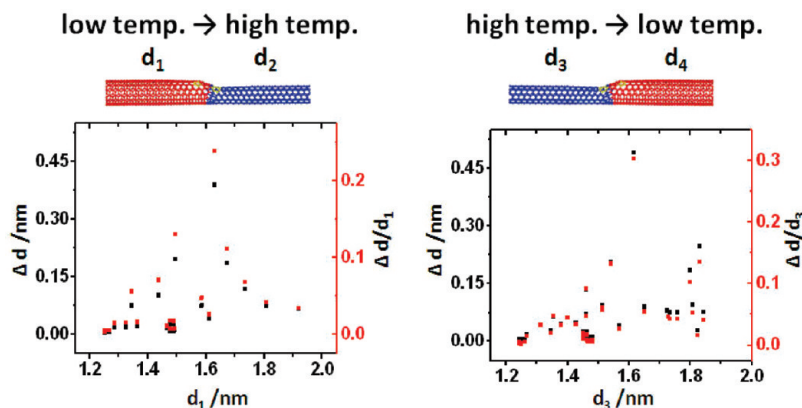
Figure 3. The relationship between the change of diameter and the initial diameter: (a) from low temperature to high temperature ($\Delta d = |d_2 - d_1|$); (b) from high temperature to low temperature ($\Delta d = |d_4 - d_3|$).
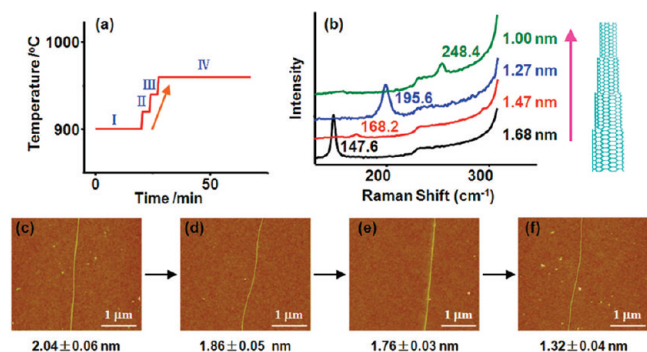
Figure 4. (a) The ascending temperature−time curve and (b) typical Raman result of an ultralong SWNT grown under the temperature−time process in panel a. The locations where the red, blue and green curves are detected are 300, 1800, and 7850 μm away from the place where the black curve is detected. The inset shows a schematic tapered structure of this SWNT. (c−f) AFM characterization of another ultralong SWNT, and the diameters measured by AFM changed from 2.04 ± 0.06 to 1.86 ± 0.05, then to 1.76 ± 0.03, and finally to 1.32 ± 0.04 nm at which it remained steady. Each of these diameters (2.04, 1.86, 1.76, and 1.32 nm) is the arithmetic mean of nearly 50 height measurements. Each of the numbers following (0.06, 0.05, 0.03, and 0.04 nm) is the standard deviation of those height measurements.

converge to 1.2 nm during the temperature oscillation range. In conclusion, the mean diameter of the SWNTs will approach 1.2 nm and even smaller if the temperature changes sufficiently, and SWNTs with a narrower diameter distribution will be obtained.

To test our reasoning discussed above, we designed a temperature ascending process to grow smaller diameter distribution SWNTs under a four-segment temperature-increase process shown in Figure 4a. In this experiment, individual ultralong SWNTs are successfully synthesized and go through different growth temperature during the whole growth stage. Thus, the ultralong SWNTs can be divided into four different segments, each of which may have different diameters. But it is still hard to characterize the diameter difference in individual SWNT especially for small difference. Although a high-resolution transmission electron microscope (TEM) can give direct evidence, it is difficult to use this method because of the complicated sample preparation. As a result, Raman RBM shift was used to offer a more precise measurement of the diameter difference. Figure 4b shows a typical Raman spectroscopy characterization result of an as-produced ultralong SWNT with four different segments and presents the diameters calculated with the equation $d = 248 \text{ cm}^{-1}/\omega_{RBM}$. When the growth temperature is increased from 900 to 920 then to 940 and 960

°C ultimately, Raman mapping along a SWNT shows that the RBM signal (G-band is shown in Supporting Information) shifts from 147.6 to 168.2, then to 195.6, finally to 248.4 cm^{-1}, which corresponds to diameters of 1.68, 1.47, 1.27, and 1.00 nm, respectively. As we expected, the diameter change trend discussed above recurs in this experiment. The inset in Figure 4b shows a schematic tapered structure based on the obtained RBM data. The RBM signals collected at each segment are undergoing slight change in frequency (within error range of the Raman system) and relative intensity, which might be caused by localized variation in the SWNT energy levels, resulting from the existence of localized defect sites or inhomogeneous environment interactions.[53,54] Additionally, there is no observable D-band (shown in Figure S2, Supporting Information), demonstrating the high quality of these SWNTs. As another conclusion, the growth rates of each segment can be calculated based on the length of each segment measured by Raman and its growth time, while the rate is 5−20 μm/s, which is consistent with the results in other works.[46,48]

In fact, we measured many SWNTs and finally found four RBM shifts along one SWNT just using single laser energy of 1.96 eV. We made great efforts in preparing for the Raman data, because the probability to find an individual SWNT with RBM signals in all four segments along one SWNT is below 1%. An important experimental phenomenon, which should be stated, is that if the number of RBM signals in an individual ultralong SWNT is two, three, or four, the RBM wavelength of the latter segment is always bigger than that of the former one. That is to say, the diameters in the latter segment are smaller than that of the former one. The Raman data cited above are all mapped along an individual SWNT following their growth direction.

To enhance the creditability of experiment under a simple ascending temperature CVD, we collected supplementary data by AFM. Figure 4c−f shows a representative AFM result. Clearly, the diameters measured change from 2.04 ± 0.06 to 1.86 ± 0.05, then to 1.76 ± 0.03, and finally to 1.32 ± 0.04 nm at which they remained steady. This result is coherent with the RBM data. All above results indicate that the diameter of a growing SWNT becomes smaller at higher temperature, even though the catalyst particle at the growing end remains the same.

Despite the diameter change along certain nanotubes proven above, we still collected the statistical data of our sample to present the overall trend of the diameter contraction. Thus, diameter distributions of the ultralong SWNTs are detected by Raman at different distance of 1.0, 2.0, and 4.0 mm from the pre-prepared catalyst line (shown in Figure 5a). The data shown
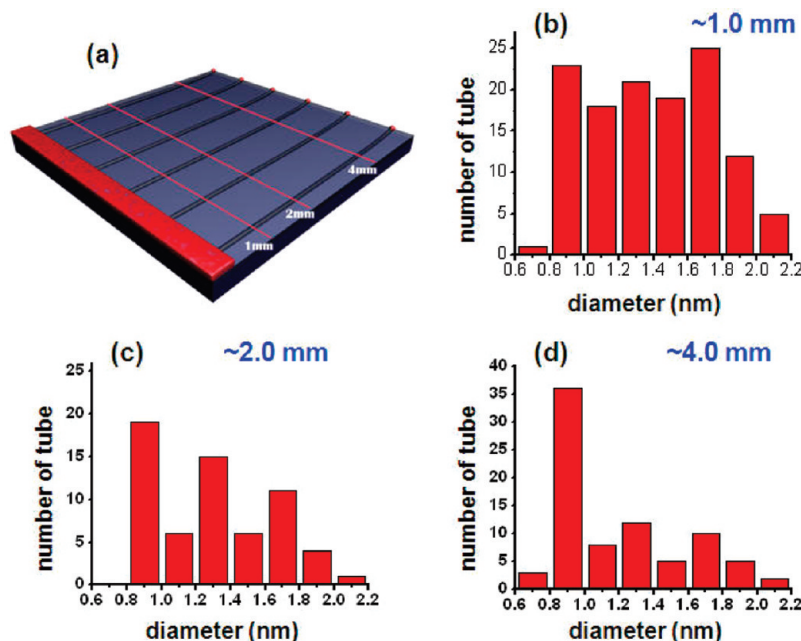
Figure 5. SWNT diameter distribution of different distance from the catalyst line grown under the temperature−time process in Figure 4a.

in Figure 5b−d illustrate clearly that the mean diameters of SWNTs far away from the catalyst line are smaller than the mean diameters of those SWNTs near it. Besides, the further from the catalyst line the diameters are measured, the narrower the diameter distribution curve is. Both of these phenomena are consistent with the aforementioned results under the presumption that usually the segments of the SWNTs close to the catalyst line are earlier grown at lower temperature, while the distant segments from the catalyst line are later synthesized at higher temperature.

According to Figure 5b−d, the total amount of data collected varies at different distances; hence the ratio of the tubes in each diameter range but not the exactly quantity would be available to offer the information of diameter distribution change. In comparison of panels b, c and d of Figure 5, the ratio of nanotubes with a larger diameter diminishes remarkably while the ratio of nanotubes with a diameter near 1.0 nm increases. Besides, the extent that the ratio of nanotubes in different diameter ranges change is consistent with Figure 3 that the diameter of nanotubes with an initial diameter around 1.6 nm is much more sensitive to temperature than that of nanotubes with an approximately 1.0 nm initial diameter. Additionally, the proportion of nanotubes with diameters above 1.2 nm in Figure 5d cannot be neglected, which may be caused by two reasons: (1) As we discussed above, the SWNTs with an initial diameter slightly larger than 1.6 nm will first approach 1.6 nm and then might be not able to reach 1.2 nm rapidly enough with our temperature oscillation range, and the SWNTs with a quite large initial diameter will also be not able to approach to 1.2 nm; thus both these groups of nanotubes would be widely distributed in various diameters from 1.2 to 2.0 nm, as shown in Figure 5d. (2) As for the presumption we mentioned in the last paragraph, which is not always true, there is a small proportion of nanotubes that grow across all the 1.0, 2.0, and 4.0 mm lines within only one or two temperature segments, despite most nanotubes undergoing the whole temperature variation stage when they grow across those lines. Although there are several defects presented above, the diameter distribution curve is successfully contracted through ascending temperature control, and we finally found a way to obtain the narrow

diameter distributed SWNTs, which would be excellent materials for AFM tips and field emitters.

To validate the opposite aspect of our conclusion, we redid the temperature-mediated CVD growth experiment under a cooling process shown in Figure 6a to obtain larger diameter SWNTs. In this experiment, the individual ultralong SWNTs with four clear segments of different diameters that are grown under different growth temperature stages are also obtained successfully. To measure the diameters of SWNTs within these four segments, Raman mapping is used to characterize the sample. As shown in Figure 6a,b, when the growth temperature decreases from 960 to 940, then to 920, finally to 900 °C, the Raman mapping results along a SWNT provide the RBM signal shift from 204.6 to 195.3, 191.3, and 169.2 cm^{-1} (G-band is shown in Supporting Information), which corresponds to diameters of 1.22, 1.27, 1.30, and 1.47 nm, respectively, the same as the trend we predicted. The figure of four segments with flared structure in an individual tube (shown in the inset of Figure 6b), which accords with the temperature change well, is given to illustrate the profile schematically. The absence of D-band signals also ensures the high quality of these SWNTs. As we discussed above, since the probability to find an individual SWNT with RBM signals in all four segments is extremely low, it still took us great effort to prepare for these Raman data. As for the individual ultralong SWNTs with two, three, or four segments that have RBM signals, the RBM wavelength of the latter segment is always smaller than that of the former one that is similar with the case above. The Raman data are all mapped along individual SWNTs following their growth direction.

We also chose a SWNT whose diameter change could be clearly distinguished by AFM, and the AFM results are shown in Figure 6c−f. The diameters are 1.34 ± 0.04, 1.45 ± 0.03, 1.69 ± 0.04, and 1.98 ± 0.05 nm, corresponding to different growth temperatures in different segments. The same as the case in our last experiment, this result is also accordant with the RBM data. All above results indicate that the diameter of a growing SWNT becomes larger at lower temperature. As a result, this phenomenon provides us a method to obtain the narrowly distributed SWNTs of large diameters, through long-playing
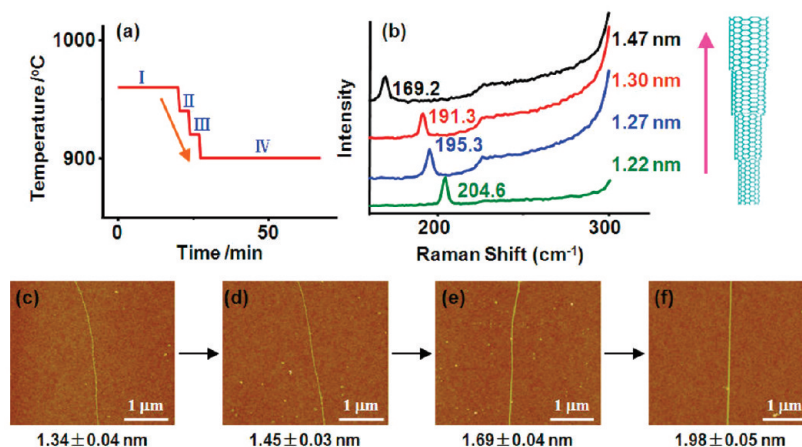
Figure 6. (a) The descending temperature−time curve and (b) typical Raman result of an ultralong SWNT grown under the temperature−time process in panel a. The locations where the blue, red, and black curves are detected are 500, 1750, and 8400 μm away from the place where the green curve is detected. The inset shows schematic flared structure of this SWNT. (c−f) AFM characterization of another ultralong SWNT; the diameters measured by AFM changed from 1.34 ± 0.04 (c) to 1.45 ± 0.03 (d), then to 1.69 ± 0.04 (e), and finally to 1.98 ± 0.05 nm, remaining steady (f), which corresponds to different segments in different growth temperature. Each of these diameters (1.34, 1.45, 1.69, and 1.98 nm) is the arithmetic mean of nearly 50 height measurements. Each of the numbers following (0.04, 0.03, 0.04, and 0.05 nm) is the standard deviation of those height measurements.

descending temperature-mediated CVD. These large diameter SWNTs can provide sufficient band gaps for high on/off ratios, enhanced high carrier mobility, ballistic transport, and high compatibility with high-κ dielectrics, and allow them to become proper materials for good near-Ohmic electrical contacts and, therefore, to be expected to exhibit high performance for nanoelectronics.[58]

To enhance the authenticity of the temperature tune effect on the diameters of SWNTs, we should prove the precondition that the ultralong SWNTs grown without temperature change do not have diameter change. One might postulate that carbon nanotubes could show diameter changes caused by defects with no intentional temperature changes introduced. However, carbon nanotubes grown in our system have few defects. First, we used alcohol as the carbon source. The use of alcohol could reduce the impurity because much less formation of soot, or solid carbon, is known from an alcohol flame compared with that from a hydrocarbon flame.[59,60] Second, the appropriate growth temperature, usually around 920 °C, plays a key role in reducing amorphous carbon. Third, the absence of D-band of the carbon nanotubes grown in our system demonstrates the high quality of these carbon nanotubes, excluding the possibility that the diameter change is due to defects in the nanotubes. So we are convinced that no diameter change naturally occurs in the ultralong SWNT growth caused by some sort of defects. What is more, as we presented earlier, the SWNTs produced without temperature change showed a uniform Raman spectroscopy without variation beyond error range along the tubes. In addition, the SWNTs produced with one-time temperature change from 900 to 950 °C or from 950 to 900 °C in our last paper showed only one sharp G-band and RBM changed. From the evidence above, we are assured that the diameter change did not happen naturally along the length of the regular long SWNTs.

Another phenomenon should be also mentioned here. Among the AFM data and Raman data shown in Figures 4b−f, and 6b−f, the diameter of nanotubes with an initial diameter around 1.6 nm is much more sensitive to temperature than that of the nanotubes with larger or smaller initial diameters. First, in Figure 4c−f, the nanotubes with initial diameters of 2.04, 1.86, and 1.76 nm change their diameter by 0.18, 0.10, and 0.44 nm, respectively. The nanotubes with the initial diameter mostly near

by 1.6 nm change most. Second, in Figure 6b, the nanotubes with initial diameters of 1.22, 1.27, and 1.30 nm change their diameter by 0.05 nm, 0.03 and 0.17 nm, respectively. It is still coherent with the trend we predicted that the nanotubes with the initial diameter mostly near 1.6 nm change most. Third, in Figure 6c−f, the nanotubes with initial diameters of 1.34, 1.45, and 1.69 nm change their diameter by 0.11, 0.24, and 0.29 nm, respectively, which also show the same phenomenon. Fourthly, in Figure 4b, the nanotubes with initial diameters of 1.68, 1.47, and 1.27 nm change their diameters by 0.21, 0.20, and 0.27 nm, respectively. For the nanotubes with these different initial diameters, the extent they change is nearly the same. This abnormal data might be caused by the unclear trend being submerged by the instrumental error and other factors such as the carbon source pressure fluctuation caused by temperature oscillation. Besides, the diameter change extent of 0.21 and 0.20 nm for the nanotubes with initial diameters of 1.68 and 1.47 nm may not be the maximum diameter change for the nanotubes with the same initial diameters. As we discussed before Figure 3, there are various probabilities of different diameter changes, but all of them are below a certain maximum of 0.40 nm for the nanotubes with an initial diameter around 1.6 nm. In addition, in Figure 5, the same case happens, and the detailed analysis has been presented above.

C. Growth Model of SWNTs. How and why could the growth parameters, especially temperature, tune the tube diameter? Some research of in situ studies of the formation of the nanotubes might explore the crucial growth parameter that may modulate the diameters of SWNTs, but it is still immature; thus the exact mechanism that the nanotube growth actually undergoes is not available so far. We believe that an assumed model of the growth of SWNTs could be important for the understanding of the experimentally observed dependences of the SWNTs' diameters on the experimental parameters; besides it is also a useful tool to help find appropriate reaction parameters to synthesize SWNTs of certain diameter distributions that are required for special applications. Ding et al. also proposed that computational modeling of the growth process plays an important role in deepening the understanding of the SWNT growth mechanism at the atomic level.[61] Therefore, it is interesting to explore the growth parameters for modulating

Tuning Diameter of Single-Walled Carbon Nanotubes

J. Phys. Chem. C, Vol. 113, No. 30, 2009 **13057**
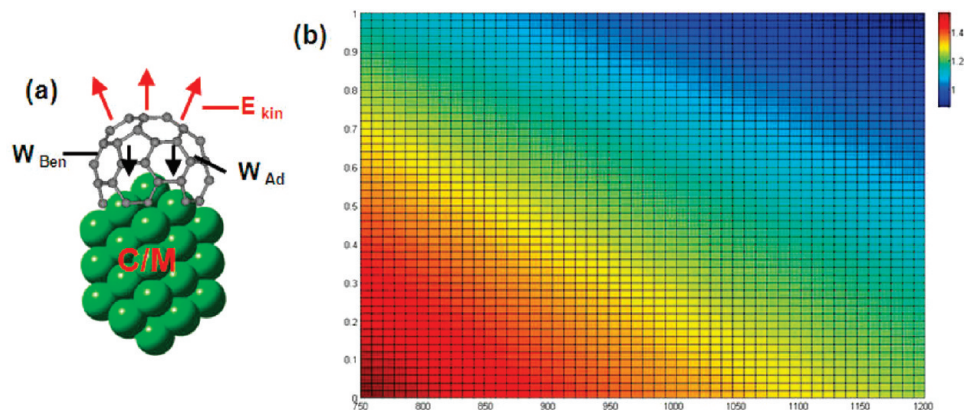
Figure 7. (a) Model of the graphene transition state and catalyst nanoparticle and (b) calculated SWNT diameter distribution at temperature between 750 and 1200 °C and mole fraction of carbon between 0 and 1.

the diameters of the SWNTs both theoretically and experimentally. Thus, we absolutely adopted the growth model and the equations (eq 1−7) proposed by Kanzow and his coworkers to probe into the relationship between the tube diameters and experimental parameters especially the growth temperature.[62,63] In this model, by assuming a graphene transition state when tube formation is initiated, graphene sheets are first nucleated from the surface of a liquid catalyst particle and then form fullerene-like caps, as shown in Figure 7a. To form graphene sheets favorably, the effective average kinetic energy, E_{kin}, per area on the particle−graphene interface must be greater than the work of adhesion, W_{Ad}, per area in the graphitic sheet toward the catalyst particle (eq 1):

$$E_{kin} - W_{Ad} \geq 0 \qquad (1)$$

The growth of SWNTs can only happen if the excess energy is used for overcoming the energy of bending the graphene sheet per area W_{Ben} (eq 2). In order to calculate eq 2, we used the formula, equations, and constants[62−65] that are partially exhibited in eqs 3−7. The parameters used in eqs 1−7 are defined in the Supporting Information.

$$W_{Ben} = E_{kin} - W_{Ad} \qquad (2)$$

$$E_{kin} = kT/A_C + kT/A_{MC} \qquad (3)$$

$$W_{Ben} \approx \Delta H_f/A_C - 2E_{S,G} = e[A + B \ln(\pi d^2/A_C)]/(\pi d^2) - 2E_{S,G} \qquad (4)$$

$$A_{MC} \approx [X_C a_{C-C} + (1 - X_C)a_{M-M}]^2 \qquad (5)$$

$$W_{Ad,G} \approx 2E_{S,G} \qquad (6)$$

$$E_{S,G} = -5.85 \times 10^{-5}T + 0.15 \ \text{J} \cdot \text{m}^{-2} \qquad (7)$$

Then we set the carbon mole fraction to be between 0 and 1 and the temperature between 750 and 1200 °C, and the calculated result is shown in Figure 7b, which indicates that (1) the higher the growth temperature, the smaller the tube diameter and (2) the smaller the mole fraction of carbon in the surface of the catalytic particle, the larger the tube diameter.

As adequate carbon source is applied, the catalyst particle should be saturated with carbon; hence the molefraction of carbon in a certain catalytic particle would not vary during the growth process. Under this precondition, the diameter of the SWNT would decrease at higher temperature and increase at lower temperature following the computational conclusion, and this trend accords well with the above experimental data we obtained. Moreover, these two calculated results have not been reported as far as we know, and the tendency of diameter change with the temperature change is also different from the results proposed by others.

What is the reason for the correlation between the calculation and experimental results? Equations 2−7 clearly demonstrate that if the kinetic energy is only slightly larger than adhesion energy per area, the excess energy available in the system is limited; thus the graphene sheet has to be rolled into a large diameter bucket structure in order to reduce the bending energy of the graphene sheet per area; if the energy excess is large and positive, a big curvature can be reached and nanotubes with small diameters will be formed. When the temperature increases, it is easy to find that the two items E_{kin} and $-W_{Ad}$ in the right side of eq 2 are both increased, that is to say, there is more excess energy to overcome the barrier of bending a small area of graphene sheet into a bucket structure, which will finally result in the formation of smaller diameter SWNTs.

Another point that should be mentioned here is that the general diameter of SWNTs that we obtained in experiments is 1.0−2.0 nm and the diameter range of SWNTs that we calculated when $X_C = 0-1$ and $T = 900-960$ °C is 1.0−1.4 nm. Why are there many SWNTs with a diameter much larger than the calculated results under our growth condition? We thought that the reason should be the validity of eq 2, which denotes that the excess energy of average kinetic energy, E_{kin}, over the work of adhesion, W_{Ad}, is used for overcoming the energy of bending the graphene sheet per area W_{Ben}. However, no evidence shows that the excess energy is totally used to offset the bending work, and it is also possible for the excess energy to be transferred into other forms such as heat and the extra energy required by the occurrence of defects besides the energy of bending. Therefore the actual bending energy should be part of the excess energy between E_{kin} and W_{Ad} and thus smaller than our computational results discussed above. SWNTs with a variety of diameters are possibly formed, if only the excess energy between E_{kin} and W_{Ad} is larger than the bending energy. That is to say the real diameters of SWNTs produced in our system should be either probably fit to or larger than our calculated results. In addition, the model is simple, and we

introduced many rough approximations to perform this calculation. The values of the work of adhesion have some experimental uncertainties. We also neglected other aspects that might influence the diameters besides the growth temperature and the mole fraction of carbon.

Conclusion

In summary, we have demonstrated that the diameter of SWNTs grown via a CVD system could be tuned by temperature and the SWNTs grown from the same catalyst particle become thinner when we increase the growth temperature and become thicker when we decrease it. In the temperature changing growth process, we also found that the diameter changes are tightly related to their initial diameters. For each initial diameter, there are various probabilities of different diameter changes, but all of them are below a certain maximum, which depends on the initial diameter. The maximum diameter change exhibits a peaked curve depending on the initial diameter and reaches an extreme of 0.40 nm when the initial diameter is around 1.6 nm. Based on this result, we designed ascending or descending temperature-mediated CVD to obtain a well-aligned individual ultralong SWNT array with a narrow diameter distribution of small diameter or larger diameter. By this method, it is feasible to grow SWNTs with tunable diameters in the different areas away from the catalyst line, which opens up a valuable way to make large-scale carbon nanotube-based devices and circuits. In the meantime, a simple growth model assuming that there is a graphene transition state at the beginning of the formation of nanotubes was provided to explain these phenomena. Under this model, the relationship between the growth temperature and the diameter of SWNTs was calculated, which indicates that a catalyst particle with a certain mole fraction of carbon will produce a SWNT with smaller diameter under higher growth temperature and a larger diameter under lower temperature. This trend accords well with our experimental data. Such diameter modulation of SWNTs by temperature would also help us to understand the CVD growth mechanism of SWNTs.

Supporting Information Available: Typical temperature oscillation between 900 and 950 °C, G-band and D-band of Raman spectroscopy, table of part of SWNTs investigated through Raman spectroscopy, and definitions for the parameters used in eqs 1−7. This material is available free of charge via the Internet at http://pubs.acs.org.

References and Notes

(1) Baughman, R. H.; Zakhidov, A. A.; de Heer, W. A. *Science* **2002**, *297*, 787–792.

(2) Avouris, P.; Chen, Z. H.; Perebeinos, V. *Nat. Nanotechnol.* **2007**, *2*, 605–615.

(3) Odom, T. W.; Huang, J. L.; Kim, P.; Lieber, C. M. *Nature* **1998**, *391*, 62–64.

(4) Iijima, S.; Ichihashi, T. *Nature* **1993**, *363*, 603–605.

(5) Bethune, D. S.; Kiang, C. H.; Devries, M. S.; Gorman, G.; Savoy, R.; Vazquez, J.; Beyers, R. *Nature* **1993**, *363*, 605–607.

(6) Thess, A.; Lee, R.; Nikolaev, P.; Dai, H. J.; Petit, P.; Robert, J.; Xu, C. H.; Lee, Y. H.; Kim, S. G.; Rinzler, A. G.; Colbert, D. T.; Scuseria, G. E.; Tomanek, D.; Fischer, J. E.; Smalley, R. E. *Science* **1996**, *273*, 483–487.

(7) Hata, K.; Futaba, D. N.; Mizuno, K.; Namai, T.; Yumura, M.; Iijima, S. *Science* **2004**, *306*, 1362–1364.

(8) http://en.wikipedia.org/wiki/Carbon_nanotube.

(9) Ren, Z. F.; Huang, Z. P.; Xu, J. W.; Wang, J. H.; Bush, P.; Siegal, M. P.; Provencio, P. N. *Science* **1998**, *282*, 1105–1107.

(10) Li, B.; Goh, C. F.; Zhou, X. Z.; Lu, G.; Tantang, H.; Chen, Y. H.; Xue, C.; Y. C. Boey, F.; Zhang, H. *Adv. Mater.* **2008**, *20*, 4873–4878.

(11) Kong, J.; Soh, H. T.; Cassell, A. M.; Quate, C. F.; Dai, H. J. *Nature* **1998**, *395*, 878–881.

(12) Huang, S. M.; Cai, X. Y.; Liu, J. *J. Am. Chem. Soc.* **2003**, *125*, 5636–5637.

(13) Fan, S. S.; Chapline, M. G.; Franklin, N. R.; Tombler, T. W.; Cassell, A. M.; Dai, H. J. *Science* **1999**, *283*, 512–514.

(14) Campidelli, S.; Meneghetti, M.; Prato, M. *Small* **2007**, *3*, 1672–1676.

(15) Strano, M. S.; Dyke, C. A.; Usrey, M. L.; Barone, P. W.; Allen, M. J.; Shan, H. W.; Kittrell, C.; Hauge, R. H.; Tour, J. M.; Smalley, R. E. *Science* **2003**, *301*, 1519–1522.

(16) Zhang, G. Y.; Qi, P. F.; Wang, X. R.; Lu, Y. R.; Li, X. L.; Tu, R.; Bangsaruntip, S.; Mann, D.; Zhang, L.; Dai, H. J. *Science* **2006**, *314*, 974–977.

(17) Huang, H. J.; Maruyama, R.; Noda, K.; Kajiura, H.; Kadono, K. *J. Phys. Chem. B* **2006**, *110*, 7316–7320.

(18) Zhang, Y. Y.; Zhang, Y.; Xian, X. J.; Zhang, J.; Liu, Z. F. *J. Phys. Chem. C* **2008**, *112*, 3849–3856.

(19) Collins, P. C.; Arnold, M. S.; Avouris, P. *Science* **2001**, *292*, 706–709.

(20) Zheng, M.; Semke, E. D. *J. Am. Chem. Soc.* **2007**, *129*, 6084–6085.

(21) Zheng, M.; Jagota, A.; Strano, M. S.; Santos, A. P.; Barone, P.; Chou, S. G.; Diner, B. A.; Dresselhaus, M. S.; McLean, R. S.; Onoa, G. B.; Samsonidze, G. G.; Semke, E. D.; Usrey, M.; Walls, D. J. *Science* **2003**, *302*, 1545–1548.

(22) Arnold, M. S.; Stupp, S. I.; Hersam, M. C. *Nano Lett.* **2005**, *5*, 713–718.

(23) Chattopadhyay, D.; Galeska, L.; Papadimitrakopoulos, F. *J. Am. Chem. Soc.* **2003**, *125*, 3370–3375.

(24) Arnold, M. S.; Green, A. A.; Hulvat, J. F.; Stupp, S. I.; Hersam, M. C. *Nat. Nanotechnol.* **2006**, *1*, 60–65.

(25) Krupke, R.; Hennrich, F.; von Lohneysen, H.; Kappes, M. M. *Science* **2003**, *301*, 344–347.

(26) Bhaviripudi, S.; Mile, E.; Steiner, S. A.; Zare, A. T.; Dresselhaus, M. S.; Belcher, A. M.; Kong, J. *J. Am. Chem. Soc.* **2007**, *129*, 1516–1517.

(27) Cheung, C. L.; Kurtz, A.; Park, H.; Lieber, C. M. *J. Phys. Chem. B* **2002**, *106*, 2429–2433.

(28) Lu, C. G.; Liu, J. *J. Phys. Chem. B* **2006**, *110*, 20254–20257.

(29) Wang, B.; Poa, C. H. P.; Wei, L.; Li, L. J.; Yang, Y. H.; Chen, Y. *J. Am. Chem. Soc.* **2007**, *129*, 9014–9019.

(30) Zhang, G. Y.; Mann, D.; Zhang, L.; Javey, A.; Li, Y. M.; Yenilmez, E.; Wang, Q.; McVittie, J. P.; Nishi, Y.; Gibbons, J.; Dai, H. J. *Proc. Natl. Acad. Sci. U.S.A.* **2005**, *102*, 16141–16145.

(31) Chen, Y.; Ciuparu, D.; Lim, S.; Yang, Y. H.; Haller, G. L.; Pfefferle, L. *J. Catal.* **2004**, *226*, 351–362.

(32) Fu, Q.; Huang, S. M.; Liu, J. *J. Phys. Chem. B* **2004**, *108*, 6124–6129.

(33) Lu, J.; Yi, S. S.; Kopley, T.; Qian, C.; Liu, J.; Gulari, E. *J. Phys. Chem. B* **2006**, *110*, 6655–6660.

(34) An, L.; Owens, J. M.; McNeil, L. E.; Liu, J. *J. Am. Chem. Soc.* **2002**, *124*, 13688–13689.

(35) Li, Y. M.; Kim, W.; Zhang, Y. G.; Rolandi, M.; Wang, D. W.; Dai, H. J. *J. Phys. Chem. B* **2001**, *105*, 11424–11431.

(36) Choi, H. C.; Kim, W.; Wang, D. W.; Dai, H. J. *J. Phys. Chem. B* **2002**, *106*, 12361–12365.

(37) Chen, Y.; Wei, L.; Wang, B.; Lim, S. Y.; Ciuparu, D.; Zheng, M.; Chen, J.; Zoican, C.; Yang, Y. H.; Haller, G. L.; Pfefferle, L. D. *ACS Nano* **2007**, *1*, 327–336.

(38) Ciuparu, D.; Chen, Y.; Lim, S.; Haller, G. L.; Pfefferle, L. *J. Phys. Chem. B* **2004**, *108*, 503–507.

(39) Ago, H.; Imamura, S.; Okazaki, T.; Saitoj, T.; Yumura, M.; Tsuji, M. *J. Phys. Chem. B* **2005**, *109*, 10035–10041.

(40) Bandow, S.; Asaka, S.; Saito, Y.; Rao, A. M.; Grigorian, L.; Richter, E.; Eklund, P. C. *Phys. Rev. Lett.* **1998**, *80*, 3779–3782.

(41) Liu, Q. F.; Ren, W. C.; Chen, Z. G.; Wang, D. W.; Liu, B. L.; Yu, B.; Li, F.; Cong, H. T.; Cheng, H. M. *ACS Nano* **2008**, *2*, 1722–1728.

(42) Smalley, R. E.; Li, Y. B.; Moore, V. C.; Price, B. K.; Colorado, R.; Schmidt, H. K.; Hauge, R. H.; Barron, A. R.; Tour, J. M. *J. Am. Chem. Soc.* **2006**, *128*, 15824–15829.

(43) Yao, Y. G.; Li, Q. W.; Zhang, J.; Liu, R.; Jiao, L. Y.; Zhu, Y. T.; Liu, Z. F. *Nat. Mater.* **2007**, *6*, 283–286.

(44) Hofmann, S.; Csanyi, G.; Ferrari, A. C.; Payne, M. C.; Robertson, J. *Phys. Rev. Lett.* **2005**, *95*, 036101.

(45) Jin, Z.; Chu, H. B.; Wang, J. Y.; Hong, J. X.; Tan, W. C.; Li, Y. *Nano Lett.* **2007**, *7*, 2073–2079.

Tuning Diameter of Single-Walled Carbon Nanotubes

J. Phys. Chem. C, Vol. 113, No. 30, 2009 **13059**

(46) Zheng, L. X.; O'Connell, M. J.; Doorn, S. K.; Liao, X. Z.; Zhao, Y. H.; Akhadov, E. A.; Hoffbauer, M. A.; Roop, B. J.; Jia, Q. X.; Dye, R. C.; Peterson, D. E.; Huang, S. M.; Liu, J.; Zhu, Y. T. *Nat. Mater.* **2004**, *3*, 673–676.

(47) Hofmann, M.; Nezich, D.; Reina, A.; Kong, J. *Nano Lett.* **2008**, *12*, 4122–4127.

(48) Yao, Y. G.; Liu, R.; Zhang, J.; Jiao, L. Y.; Liu, Z. F. *J. Phys. Chem. C* **2007**, *111*, 8407–8409.

(49) Huang, L.; White, B.; Sfeir, M. Y.; Huang, M.; Huang, H. X.; Wind, S.; Hone, J.; O'Brien, S. *J. Phys. Chem. B* **2006**, *110*, 11103–11109.

(50) Hong, B. H.; Lee, J. Y.; Beetz, T.; Zhu, Y. M.; Kim, P.; Kim, K. S. *J. Am. Chem. Soc.* **2005**, *127*, 15336–15337.

(51) Huang, S. M.; Woodson, M.; Smalley, R.; Liu, J. *Nano Lett.* **2004**, *4*, 1025–1028.

(52) Zhang, Y.; Zhang, J.; Son, H.; Kong, J.; Liu, Z. *J. Am. Chem. Soc.* **2005**, *127*, 17156–17157.

(53) Doorn, S. K.; Zheng, L.; O'Connell, M. J.; Zhu, Y.; Huang, S.; Liu, J. *J. Phys. Chem. B* **2005**, *109*, 3751–3758.

(54) Doorn, S. K.; O'Connell, M. J.; Zheng, L. X.; Zhu, Y. T. T.; Huang, S. M.; Liu, J. *Phys. Rev. Lett.* **2005**, *94*, 016802.

(55) Dresselhaus, M. S.; Dresselhaus, G.; Jorio, A.; Souza, A. G.; Saito, R. *Carbon* **2002**, *40*, 2043–2061.

(56) Dresselhaus, M. S.; Dresselhaus, G.; Jorio, A. *J. Phys. Chem. C* **2007**, *111*, 17887–17893.

(57) Jorio, A.; Saito, R.; Hafner, J. H.; Lieber, C. M.; Hunter, M.; McClure, T.; Dresselhaus, G.; Dresselhaus, M. S. *Phys. Rev. Lett.* **2001**, *86*, 1118–1121.

(58) Kim, W.; Javey, A.; Tu, R.; Cao, J.; Wang, Q.; Dai, H. J. *Appl. Phys. Lett.* **2005**, *87*, 173101.

(59) Lupo, F.; Rodriguez-Manzo, J. A.; Zamudio, A.; Elias, A. L.; Kim, Y. A.; Hayashi, T.; Muramatsu, M.; Kamalakaran, R.; Terrones, H.; Endo, M.; Ruhle, M.; Terrones, M. *Chem. Phys. Lett.* **2005**, *410*, 384–390.

(60) Maruyama, S.; Kojima, R.; Miyauchi, Y.; Chiashi, S.; Kohno, M. *Chem. Phys. Lett.* **2002**, *360*, 229–234.

(61) Ding, F.; Larsson, P.; Larsson, J. A.; Ahuja, R.; Duan, H. M.; Rosen, A.; Bolton, K. *Nano Lett.* **2008**, *8*, 463–468.

(62) Kanzow, H.; Ding, A. *Phys. Rev. B* **1999**, *60*, 11180–11186.

(63) Kanzow, H.; Lenski, C.; Ding, A. *Phys. Rev. B* **2001**, *63*, 125402.

(64) Tersoff, J. *Phys. Rev. B* **1992**, *46*, 15546–15549.

(65) Zhang, B. L.; Xu, C. H.; Wang, C. Z.; Chan, C. T.; Ho, K. M. *Phys. Rev. B* **1992**, *46*, 7333–7336.